



Cite this: *J. Mater. Chem. B*, 2022, 10, 6752

## Fluorescence detection of milk allergen $\beta$ -lactoglobulin based on aptamers and WS<sub>2</sub> nanosheets†

Chengyi Hong,<sup>a</sup> Jingjing Wang,<sup>a</sup> Yuying Wang,<sup>a</sup> Zhiyong Huang,<sup>a</sup> Hongfen Yang,<sup>\*b</sup> Dan Yang,<sup>c</sup> Ren Cai<sup>\*d</sup> and Weihong Tan<sup>d</sup>

$\beta$ -Lactoglobulin ( $\beta$ -Lg), a food allergen, can easily cause allergic reactions in infants and young children. Therefore, it is necessary to develop a rapid, sensitive, and selective detection method to protect individuals prone to allergies. In this paper, a fluorescence assay based on WS<sub>2</sub> nanosheets and a fluorescent dye (FAM)-labeled  $\beta$ -Lg aptamer was designed to detect  $\beta$ -Lg rapidly with high sensitivity. In the sensing platform, the  $\beta$ -Lg aptamer is adsorbed on the WS<sub>2</sub> nanosheet surface by van der Waals forces, which trigger the phenomenon of fluorescence resonance energy transfer (FRET) and suppress the fluorescence signal in the system. When  $\beta$ -Lg is present, the conformation of the aptamer specifically bound to  $\beta$ -Lg changes. Therefore, the aptamer is separated from the WS<sub>2</sub> nanosheet surface, and the fluorescence signal is recovered. This method combines the high quenching efficiency of WS<sub>2</sub> nanosheets and good specificity of the  $\beta$ -Lg aptamer. The detection range of this method for  $\beta$ -Lg is 0.1–100  $\mu\text{g mL}^{-1}$ . The detection limit is 20.4 ng mL<sup>-1</sup>. This method exhibits high sensitivity, selectivity and good reproducibility, and it can be used for  $\beta$ -Lg detection in actual samples.

Received 5th February 2022,  
Accepted 30th March 2022

DOI: 10.1039/d2tb00263a

rsc.li/materials-b

## Introduction

Food allergy reflects the response of the human immune system to certain ingredients in food, which can result in various skin, gastrointestinal and respiratory diseases, and even endanger human life in severe cases.<sup>1</sup> In 1995, milk, eggs, peanuts, nuts, wheat, soybeans, fish, and shellfish were recognized by the Food and Agriculture Organization of the United Nations (FAO) as the eight major food categories that cause food allergies.<sup>2</sup> Milk is rich in protein, mainly casein and whey protein. Whey protein consists of  $\beta$ -lactoglobulin ( $\beta$ -Lg),  $\alpha$ -lactalbumin ( $\alpha$ -La), lactoferrin, bovine serum albumin (BSA), and immunoglobulin.<sup>3</sup>  $\beta$ -Lg accounts for about 12% of the total milk protein and 50% of the whey protein, and its

concentration in milk is 2–4 g L<sup>-1</sup>.<sup>4</sup> Meanwhile,  $\beta$ -Lg is widespread in foods due to its high nutritional value and multiple functions, e.g., foaming, gelation, binding properties, emulsification, and food additives.<sup>5,6</sup> However, many research studies have shown that proteins in milk can lead to allergic reactions in 2% to 3% of infants and young children, and that 60% to 80% of milk allergies are caused by  $\beta$ -Lg.<sup>7,8</sup> Although food labelling laws and regulations of most countries stipulate that the common allergens must be declared in the ingredient list of food packaging,<sup>9</sup> it is still difficult to avoid the mixing of allergens in food processing and packaging. Therefore, it is necessary to establish an effective  $\beta$ -Lg detection strategy to protect public health.

To date, many analytical methods have been developed to detect  $\beta$ -Lg. Traditional chromatography is commonly used for  $\beta$ -Lg monitoring, including high performance liquid chromatography (HPLC),<sup>10</sup> ultra-high performance liquid chromatography (UHPLC),<sup>11</sup> and liquid chromatography tandem mass spectrometry (LC-MS/MS).<sup>12</sup> In addition, some novel detection methods, such as enzyme-linked immunosorbent assay,<sup>13</sup> photoelectrochemical immunoassay,<sup>14</sup> lateral flow immunoassay,<sup>15</sup> real-time quantitative polymerase chain reaction,<sup>16</sup> transient isotachopheresis,<sup>17</sup> and molecular imprinting,<sup>18</sup> have also been used for the detection of  $\beta$ -Lg. Although these reported methods have exhibited very good detection sensitivity and accuracy, there are still some disadvantages, such as the need for expensive analytical equipment and

<sup>a</sup> College of Ocean Food and Biological Engineering, Fujian Provincial Key Laboratory of Food Microbiology and Enzyme Engineering, Jimei University, Xiamen, 361021, China

<sup>b</sup> University of Texas at Austin, Austin, TX 78712, USA.  
E-mail: yanghf88@gmail.com

<sup>c</sup> RMIT University, Melbourne, Australia

<sup>d</sup> Molecular Science and Biomedicine Laboratory, State Key Laboratory for Chemo/Bio-Sensing and Chemometrics, College of Chemistry and Chemical Engineering, College of Biology College of Material Science and Engineering, and Collaborative Research Center of Molecular Engineering for Theranostics, Hunan University, Changsha, 410082, China. E-mail: cairen@hnu.edu.cn

† Electronic supplementary information (ESI) available. See <https://doi.org/10.1039/d2tb00263a>

complex sample pre-treatment processes. For instance, immunoassay is costly and requires long analysis time, and the stability of antibodies is very difficult to maintain. A DNA-based polymerase chain reaction relies on specific sequences, and the equipment is expensive and the procedure is time consuming.

Aptamers are single-stranded DNA or RNA selected from a random sequence nucleic acid library through an exponential enrichment (SELEX) process, and they specifically bind to target molecules.<sup>19</sup> Compared with antibodies, aptamers possess the advantages of low cost, high stability, easy synthesis, and labelling.<sup>20</sup> Meanwhile, owing to their obvious affinity for most biomolecules, many electrochemical, colorimetric, and fluorescence methods have been extensively studied in the field of aptamer-based biomolecule detection.<sup>21,22</sup> Among them, fluorescence-based detection methods have attracted much attention due to their simplicity, speed, low cost, and high sensitivity, and been widely used in protein detection.<sup>23,24</sup> So far, there have been few fluorescence methods based on aptamers to detect  $\beta$ -Lg.<sup>25,26</sup>

In recent years, transition metal chalcogenides (e.g.,  $\text{MoS}_2$  and  $\text{WS}_2$ ) have been discovered and studied as two-dimensional (2D) nanomaterials similar to graphene oxide.<sup>27,28</sup> Compared with graphene oxide, transition metal chalcogenide nanosheets are easier to synthesize on a large scale, and can be directly dispersed in an aqueous solution without any surfactants.<sup>29–32</sup>  $\text{WS}_2$  nanosheets can recognize single-stranded DNA (ssDNA) and double-stranded DNA (dsDNA), due to the presence of van der Waals forces between the cyclic bases and  $\text{WS}_2$  nanosheets.<sup>33</sup> As a result, single-stranded DNA (ssDNA) can be adsorbed on the  $\text{WS}_2$  nanosheet surface. This feature has been applied to many fluorescence analyses<sup>34–36</sup> and makes  $\text{WS}_2$  nanosheets an ideal material for designing a fluorescence assay for  $\beta$ -Lg detection.

In this work, we exploited  $\text{WS}_2$  nanosheets to construct a fluorescence assay based on aptamer fluorescence quenching and recovery to detect  $\beta$ -Lg. In this sensing system, when there is no target, the aptamer labelled with a fluorescent dye-FAM is adsorbed on the  $\text{WS}_2$  nanosheets by van der Waals forces. The fluorescence resonance energy transfer (FRET) phenomenon occurs between the dye molecule and the  $\text{WS}_2$  nanosheets, resulting in fluorescence quenching. However, when the target  $\beta$ -Lg is present, the aptamer specifically binds to the target, inducing aptamers to form a more rigid conformation. This rigid conformation weakens the van der Waals forces between aptamers and  $\text{WS}_2$  nanosheets. Therefore, the aptamer labelled with FAM is released from the nanosheet surface, and the fluorescence signal is restored (Fig. 1). This sensing platform exhibits high sensitivity and selectivity for  $\beta$ -Lg detection, and the detection strategy has been successfully applied to actual food products.

## Experimental

### Materials and apparatus

$\text{WS}_2$  nanosheets were purchased from Nanjing XF Nano Material Tech Co., Ltd. (Nanjing, China). Bovine serum albumin (BSA), sodium chloride (NaCl), and potassium chloride (KCl) were

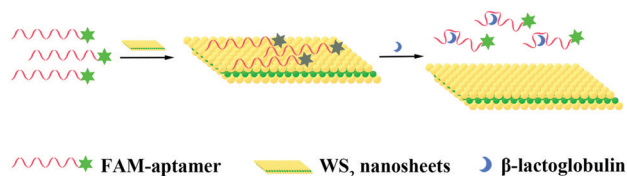


Fig. 1 Schematic diagram for detecting  $\beta$ -Lg based on aptamers and  $\text{WS}_2$  nanosheets.

purchased from Sinopharm Chemical Reagent Co., Ltd (Shanghai, China). Magnesium chloride hexahydrate ( $\text{MgCl}_2 \cdot 6\text{H}_2\text{O}$ ), and  $\gamma$ -globulin were purchased from Aladdin Biochemical Technology Co., Ltd (Shanghai, China).  $\beta$ -Lg, ovalbumin, and  $\alpha$ -lactalbumin ( $\alpha$ -La) were purchased from Sigma-Aldrich Company (Shanghai, China). Casein from bovine milk, and Tris-HCl were purchased from Shanghai Sangon Biotech Co., Ltd. Pure milk and infant formula samples were purchased from local supermarkets (Xiamen, China). The FAM labelled  $\beta$ -Lg aptamer (5'-FAM-CGACGATCGG ACCGCAGTACCCACCCACCAGCCCCAACATCATGCCCCATCCGTGT GTG-3')<sup>37</sup> was synthesized and purified by Sangon Biotech Co., Ltd (Shanghai, China). The detection buffer used in this study contained 50 mM Tris-HCl, 5 mM KCl, 100 mM NaCl, and 1 mM  $\text{MgCl}_2$ , at pH 7.4. All chemicals were of analytical grade and used without further purification. All solutions were prepared from ultrapure water obtained from a Milli-Q water purification system (Sartorius, Germany) (resistance > 18.2 M $\Omega$  cm). The fluorescence emission spectrum and fluorescence anisotropy were measured on an LS55 fluorescence spectrometer (PerkinElmer Ltd., USA). The UV-vis absorption spectrum was recorded with a Lambda 265 UV-vis spectrophotometer (PerkinElmer Ltd, USA).

### Selection of optimum reaction conditions

Typically, 120  $\mu\text{L}$   $\text{WS}_2$  nanosheets ( $200 \mu\text{g mL}^{-1}$ ) and 240  $\mu\text{L}$   $\beta$ -Lg aptamer ( $75 \text{ nmol L}^{-1}$ ) were mixed by shaking and allowed to react at room temperature. In order to determine the quenching time of the  $\beta$ -Lg aptamer by  $\text{WS}_2$  nanosheets, the fluorescence spectra at different times were recorded. Subsequently, in order to obtain the optimal response time to detect  $\beta$ -Lg, after shaking 120  $\mu\text{L}$   $\text{WS}_2$  nanosheets ( $200 \mu\text{g mL}^{-1}$ ) and 240  $\mu\text{L}$   $\beta$ -Lg aptamer ( $75 \text{ nmol L}^{-1}$ ) at room temperature for 10 min, 120  $\mu\text{L}$   $\beta$ -Lg ( $60 \mu\text{g mL}^{-1}$ ) was added to the reaction system. The reaction was carried out at 37  $^\circ\text{C}$  on a shaking table. The fluorescence spectra at different reaction times were recorded.

### $\beta$ -Lg detection

Under the optimized conditions, after the  $\beta$ -Lg aptamer and  $\text{WS}_2$  nanosheets were shaken and reacted at room temperature for 10 min, 120  $\mu\text{L}$  of  $\beta$ -Lg of various concentrations were added to the mixture, and then reacted in a shaker at 37  $^\circ\text{C}$  for 1 h. The excitation wavelength was 480 nm. The spectra were recorded between 500 and 600 nm.

### Selectivity experiment

Coexisting or similar proteins ( $\alpha$ -La, ovalbumin, BSA, casein and  $\gamma$ -globulin) were chosen as interfering substances to

evaluate the selectivity. The concentrations of interfering proteins and  $\beta$ -Lg were all  $80 \mu\text{g mL}^{-1}$ . According to the same reaction conditions described above, the effects of those several potential interfering proteins were evaluated.

### Detection of $\beta$ -Lg in food samples

The commercial pure milk and infant formula were pre-treated to avoid the influence of the food matrix on the response of the aptamer. As described in the literature,<sup>38</sup> the milk samples were heated at  $40^\circ\text{C}$  for 30 min, centrifuged at 8000 rpm for 20 min and cooled in an ice bath for 15 min. Then, the suspension was acidified with 2 M HCl to pH 4.6 for 20 min. The acidified suspension was further centrifuged at 8000 rpm for 20 min to precipitate casein. The supernatant was collected and filtered with a  $0.2 \mu\text{m}$  polycarbonate membrane. Finally, the solution was neutralized with 1 M NaOH. The pre-treated milk sample was diluted fifty-fold with the detection buffer. For the infant formula sample, 1 g milk powder was dissolved in ultrapure water (5 mL). The dissolved solution was heated to  $40^\circ\text{C}$  and held 30 min; then centrifuged at 15,000 rpm for 15 min.<sup>39</sup> The supernatant was acidified to pH 4.6 with 2 M HCl. After 20 min, the supernatant was centrifuged at 8000 rpm for 20 min. The supernatant was collected and filtered with a polycarbonate membrane (size,  $0.2 \mu\text{m}$ ). Finally, the solution was neutralized with 1 M NaOH and diluted fifty-fold with the detection buffer. Different concentrations of  $\beta$ -Lg solutions (1, 10, and  $100 \mu\text{g mL}^{-1}$ ) were added to the above solution. The determination of  $\beta$ -Lg was carried out according to the steps in  $\beta$ -Lg detection.

## Results and discussion

### Feasibility study of a fluorescence biosensing platform

First, we investigated the feasibility of the binding state of  $\text{WS}_2$  nanosheets and the FAM-labelled aptamer through the study of fluorescence anisotropy. Fluorescence anisotropy reflects the rotation ability of fluorescent molecules in the microenvironment. Therefore, it is often used to study the interactions between molecules. The adsorption of aptamers on  $\text{WS}_2$  nanosheets before and after adding the target  $\beta$ -Lg was investigated by measuring the fluorescence anisotropy of FAM. As

shown in Fig. S1 (ESI<sup>†</sup>), the fluorescence anisotropy (FA) value of the free FAM-labelled  $\beta$ -Lg aptamer in the buffer was 0.149. The value increased to 0.457 after adding  $\text{WS}_2$  nanosheets, which indicated that the FAM-labelled  $\beta$ -Lg aptamer was assembled on the  $\text{WS}_2$  nanosheet, limiting the FAM dye rotation. After adding the target  $\beta$ -Lg, the FA value decreased to 0.214, which is close to the FA value of the free FAM-labelled  $\beta$ -Lg aptamer. These results indicated that the  $\beta$ -Lg aptamer adsorbed on the  $\text{WS}_2$  nanosheet can be dissociated from the nanosheets after the reaction with  $\beta$ -Lg. After that, the FRET phenomenon in the fluorescence quenching process was verified by measuring the emission spectrum of FAM dye and the absorption spectrum of  $\text{WS}_2$  nanosheets (Fig. 2A). The absorption spectrum was mainly concentrated in the UV region, with the absorption band expanded to the near-infrared range. The overlap of the emission spectrum of the FAM dye and the absorption spectrum of  $\text{WS}_2$  nanosheets ensured the feasibility of the FRET method.

### Optimization of assay conditions for the detection of $\beta$ -Lg

To acquire the optimal sensing performance, some important parameters were optimized before detecting  $\beta$ -Lg. Because the concentration of  $\text{WS}_2$  nanosheets used in the experiment has a great influence on the fluorescence quenching reaction, we first optimized the concentration of  $\text{WS}_2$  nanosheets. As shown in Fig. 2B, as the concentration of  $\text{WS}_2$  nanosheets increased, the fluorescence intensity of the system gradually decreased. The equation for the fluorescence quenching efficiency is  $QE = (F_0 - F_q)/F_0$ , where  $F_0$  is the fluorescence intensity in the system without adding  $\text{WS}_2$  nanosheets, and  $F_q$  is the fluorescence intensity in the system quenched by  $\text{WS}_2$  nanosheets. When the concentration of  $\text{WS}_2$  nanosheets was  $200 \mu\text{g mL}^{-1}$ , the quenching efficiency reached 93%. With a further increase of the concentration of  $\text{WS}_2$  nanosheets, the fluorescence intensity was nearly unchanged. Therefore,  $200 \mu\text{g mL}^{-1}$  was taken as the optimized concentration, which ensured high quenching efficiency and a low fluorescence background signal.

In addition, by mixing the FAM-labelled  $\beta$ -Lg aptamer with the  $\text{WS}_2$  nanosheet solution, the quenching kinetics results indicated that the interaction between the aptamer and the  $\text{WS}_2$

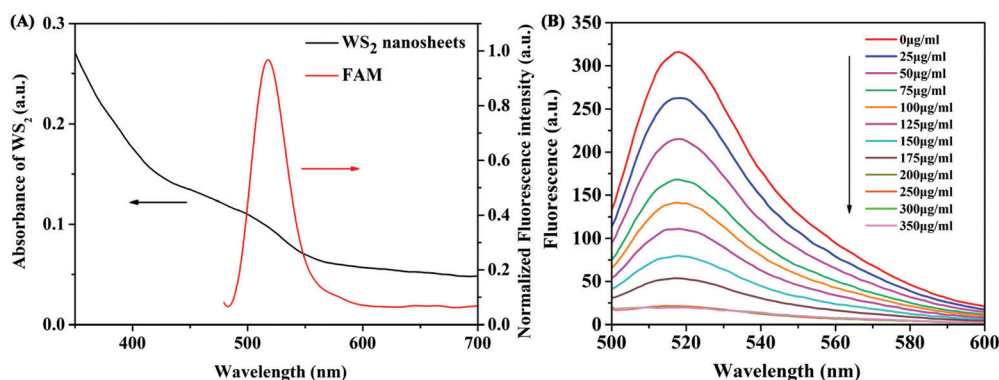


Fig. 2 (A) Spectral overlap between fluorescence emission spectra of FAM fluorescent dye and absorption spectra of  $\text{WS}_2$  nanosheets. (B) The fluorescence spectra of FAM-labelled  $\beta$ -Lg aptamers incubated with different concentrations of  $\text{WS}_2$  nanosheets.

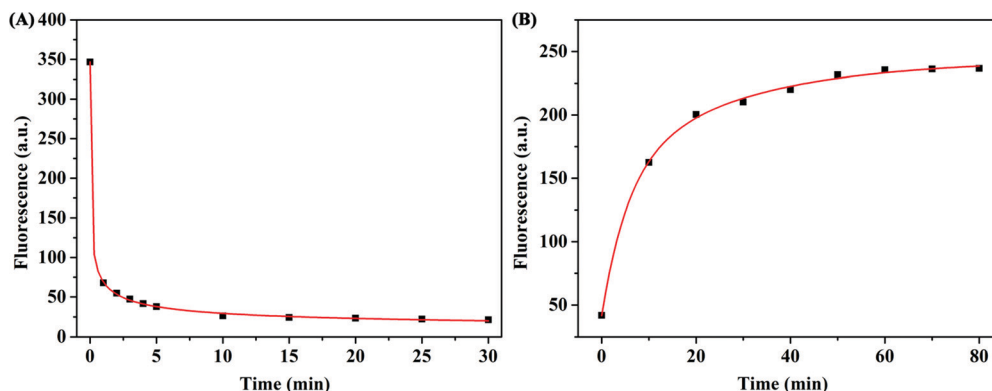


Fig. 3 (A) The fluorescence quenching effect of WS<sub>2</sub> nanosheets on FAM-labelled β-Lg aptamer changes with different reaction times. (B) Time-dependent fluorescence changes of the FAM-labelled β-Lg aptamer after adding β-Lg.

nanosheets was a fairly rapid process, reaching equilibrium within about 10 min (Fig. 3A). Therefore, 10 min was fixed as the reaction time for fluorescence quenching of the aptamer. However, after adding β-Lg to the mixture of the FAM-labelled β-Lg aptamer and WS<sub>2</sub> nanosheets, the fluorescence intensity in the reaction system gradually increased, and the fluorescence recovery equilibrium was reached after 60 min (Fig. 3B).

### Detection of β-Lg

Under the optimized detection conditions, a fluorescence assay based on WS<sub>2</sub> nanosheets and the β-Lg aptamer was established to detect β-Lg. The changes of fluorescence spectra were measured after adding different concentrations of β-Lg to FAM-complexes of the labelled β-Lg aptamer and WS<sub>2</sub> nanosheets. As shown in Fig. 4A, with increasing concentration of the target β-Lg, the fluorescence intensity of the FAM-labelled β-Lg aptamer and WS<sub>2</sub> nanosheet complexes gradually increased. The recovery of the fluorescence signal was due to the strong affinity of the aptamer for β-Lg, which caused the aptamer to desorb from the WS<sub>2</sub> nanosheet surface. As the distance between the FAM-labelled β-Lg aptamer and WS<sub>2</sub> nanosheets increased, the fluorescence signal recovered due to loss of the FRET effect.

The fluorescence intensity in the system and the concentration of β-Lg showed a good linear relationship within the range of 0.1–100 μg mL<sup>-1</sup> (Fig. 4B). The fitting equation of linear regression was  $F = 2.934C + 30.82$  ( $R^2 = 0.9911$ ), and the limit of detection (LOD) was 20.4 ng mL<sup>-1</sup>. Compared with other β-Lg detection methods, this method showed similar or better analytical performance (Table S1, ESI†). In order to evaluate the selectivity of the β-Lg detection method, we selected the same concentration of other types of proteins, *i.e.*, α-La, ovalbumin, BSA, casein and γ-globulin, as the interfering substances. As displayed in Fig. 5A, these proteins did not change the fluorescence intensity compared with β-Lg. Meanwhile, the presence of coexisting proteins had no obvious interference on the β-Lg detection (Fig. 5B). The difference of fluorescence enhancement between the β-Lg and other proteins was statistically significant ( $p < 0.001$ ) (Fig. S2, ESI†). These experimental results proved that this method has good selectivity for the β-Lg detection.

### β-Lg detection in food samples

Finally, different milk and infant formula samples were selected to study the applicability of our method in actual

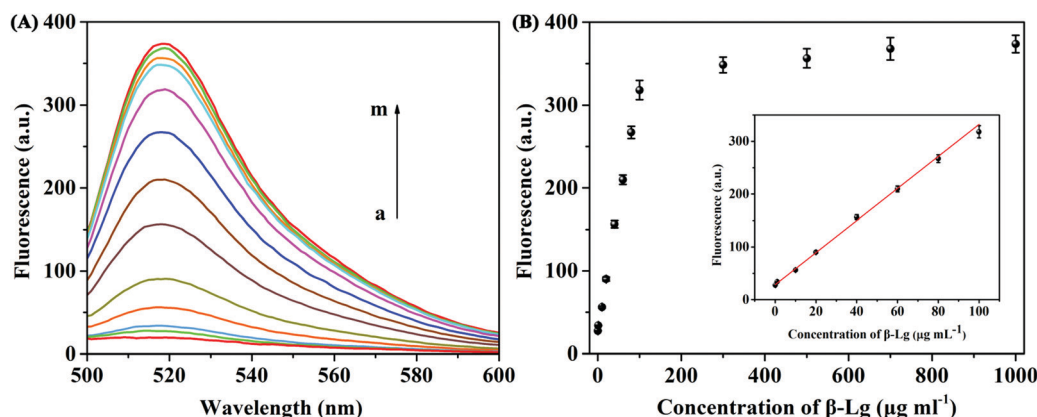


Fig. 4 (A) FAM labelled β-Lg aptamer fluorescence emission spectra of the proposed method at different concentrations of β-Lg (0, 0.1, 1, 10, 20, 40, 60, 80, 100, 300, 500, 700, and 1000 μg mL<sup>-1</sup>). (B) Diagram of peak fluorescence and target β-Lg concentration. Inset: Linear fitting of fluorescence intensity at 518 nm with the target β-Lg concentration.



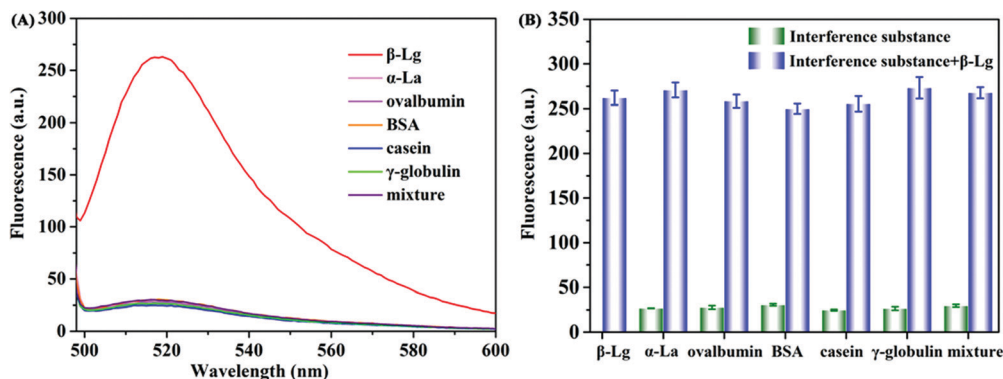


Fig. 5 Selectivity of the method. (A) Fluorescence emission spectra and (B) the fluorescence intensity at 518 nm of the system upon the addition of  $\beta$ -Lg,  $\alpha$ -Lg, ovalbumin, BSA, casein,  $\gamma$ -globulin and mixture proteins.

sample detection. In the case of the same  $\beta$ -Lg calibration curve, the content of  $\beta$ -Lg in the samples was measured by the as-developed fluorescence method. The fluorescence intensity in the system increased with the increase of the concentration of  $\beta$ -Lg. As shown in Table S2 (ESI<sup>†</sup>), the detected concentration of  $\beta$ -Lg by this method was consistent with that from commercial ELISA, and the relative standard deviation (RSD) was between 2.6% and 4.9%. The recovery rates of  $\beta$ -Lg in the spiked infant formula samples ranged from 98.1% to 103.5% (Table S3, ESI<sup>†</sup>). These experimental results showed that this method can be used to detect  $\beta$ -Lg in real samples with good precision and stability.

## Conclusions

In conclusion, we developed a simple and sensitive fluorescence method for detecting  $\beta$ -Lg based on a  $\beta$ -Lg aptamer and WS<sub>2</sub> nanosheets. The  $\beta$ -Lg aptamer was easily adsorbed on WS<sub>2</sub> nanosheets and triggered the fluorescence to be quickly quenched by the WS<sub>2</sub> nanosheets. When the target  $\beta$ -Lg was present, the fluorescence could be recovered. The detection limit was 20.4 ng mL<sup>-1</sup>, and the specificity of the detection method for  $\beta$ -Lg was superior to other interfering proteins. This fluorescence method was further applied to detect the content of  $\beta$ -Lg in actual samples, with good accuracy. Therefore, the as-developed approach shows practical application value in allergen  $\beta$ -Lg detection.

## Conflicts of interest

There are no conflicts to declare.

## Acknowledgements

This work was supported by the National Natural Science Foundation of China (21804050 and 22004032), the Natural Science Foundation of Fujian Province of China (2019J05098), and the Hunan Provincial Natural Science Foundation of China (2021JJ20020).

## Notes and references

- 1 S. H. Sicherer and H. A. Sampson, *Food Allergy*, 2010, **125**, S116–S125.
- 2 S. McClain, C. Bowman, M. Fernández-Rivas, G. S. Ladies and R. van Ree, *Clin. Transl. Allergy*, 2014, **4**, 1–9.
- 3 C. Villa, J. Costa, M. B. P. P. Oliveira and I. Mafra, *Compr. Rev. Food Sci. Food Saf.*, 2018, **17**, 137–164.
- 4 J. Y. Yin, J. S. Huo, X. X. Ma, J. Sun and J. Huang, *Biomed. Environ. Sci.*, 2017, **30**, 875–886.
- 5 B. Rullier, M. A. V. Axelos, D. Langevin and B. Novales, *J. Colloid Interface Sci.*, 2010, **343**, 330–337.
- 6 T. Nicolai, M. Britten and C. Schmitt, *Food Hydrocolloids*, 2011, **25**, 1945–1962.
- 7 J. M. Skripak, E. C. Matsui, K. Mudd and R. A. Wood, *J. Allergy Clin. Immunol.*, 2017, **120**, 1172–1177.
- 8 M. Nehra, M. Lettieri, N. Dilbaghi, S. Kumar and G. Marrazza, *Sensors*, 2020, **20**, 32.
- 9 K. J. Allen, P. J. Turner, R. Pawankar, S. Taylor, S. Sicherer, G. Lack, N. Rosario, M. Ebisawa, G. Wong, E. N. C. Mills, K. Beyer, A. Fiocchi and H. A. Sampson, *World Allergy Organ. J.*, 2014, **7**, 1–14.
- 10 O. Rotkāja, J. Goluško and P. Mekšs, *Mater. Sci. Appl. Chem.*, 2016, **33**, 36–39.
- 11 L. I. Boitz, G. Fiechter, R. K. Seifried and H. K. Mayer, *J. Chromatogr. A*, 2015, **1386**, 98–102.
- 12 J. Ji, P. Zhu, F. Pi, C. Sun, J. Sun, M. Jia, C. Ying, Y. Zhang and X. Sun, *Food Control*, 2017, **74**, 79–88.
- 13 S. He, X. Li, J. Gao, P. Tong and H. Chen, *Food Chem.*, 2017, **227**, 33–40.
- 14 C. Li, Q. Zhu, H. Chang, M. Jiang, S. Mao, Z. Chen, L. Kong, H. Liu, H. Tian and J. Wang, *J. Electroanal. Chem.*, 2021, 115964.
- 15 P. Galan-Malo, S. Pellicer, M. D. Pérez, L. Sánchez, P. Razquin and L. Mata, *Food Chem.*, 2019, **293**, 41–48.
- 16 C. Villa, J. Costa, M. B. P. P. Oliveir and I. Mafra, *Food Control*, 2010, **108**, 106823.
- 17 M. Horká, J. Šalplachta, P. Karásek and M. Roth, *Food Chem.*, 2022, 131986.
- 18 L. Hong, M. Pan, X. Yang, X. Xie, K. Liu, J. Yang, S. Wang and S. Wang, *J. Nanobiotechnol.*, 2022, **20**, 1–12.
- 19 X. Fang and W. Tan, *Acc. Chem. Res.*, 2010, **43**, 48–57.

- 20 S. Song, L. Wang, J. Li, C. Fan and J. Zhao, *TrAC, Trends Anal. Chem.*, 2008, **27**, 108–117.
- 21 C. Zhang and L. W. Johnson, *Anal. Chem.*, 2019, **81**, 3051–3055.
- 22 K. Mao, H. Zhang, Z. Wang, H. Cao, K. Zhang, X. Li and Z. Yang, *Biosens. Bioelectron.*, 2020, **148**, 111785.
- 23 Z. Chen, M. Sun, F. Luo, K. Xu, Z. Lin and L. Zhang, *Talanta*, 2018, **178**, 563–568.
- 24 S. Li, X. Liu, S. Liu, M. Guo, C. Liu and M. Pei, *Anal. Chim. Acta*, 2021, **1141**, 21–27.
- 25 S. Qi, N. Duan, Y. Sun, Y. Zhou, P. Ma, S. Wu and Z. Wang, *Sens. Actuators, B*, 2021, **340**, 129956.
- 26 M. Shi, Y. Cen, M. Sohail, G. Xu, F. Wei, Y. Ma, X. Xu, Y. Ma, Y. Song and Q. Hu, *Microchim. Acta*, 2018, **185**, 1–8.
- 27 C. H. Lu, H. H. Yang, C. L. Zhu, X. Chen and G. N. Chen, *Angew. Chem.*, 2009, **121**, 4879–4881.
- 28 D. Chimene, D. L. Alge and A. K. Gaharwar, *Adv. Mater.*, 2015, **27**, 7261–7284.
- 29 G. Chen, Y. Li, M. Bick and J. Chen, *Chem. Rev.*, 2020, **120**, 3668–3720.
- 30 N. Zhang, F. Huang, S. Zhao, X. Lv, Y. Zhou, S. Xiang, S. Xu, Y. Li, G. Chen, C. Tao, Y. Nie, J. Chen and X. Fan, *Matter*, 2020, **2**, 1260–1269.
- 31 J. Chen, Y. Huang, N. Zhang, H. Zhou, R. Liu, C. Tao, X. Fan and Z. L. Wang, *Nat. Energy*, 2016, **1**, 1–8.
- 32 X. Xiao, X. Xiao, Y. Zhou, X. Zhao, G. Chen, Z. Liu, Z. Wang, C. Lu, M. Hu, A. Nashalian, S. Shen, K. Xie, W. Wang, Y. Gong, W. Ding, P. Servati, C. Han, S. X. Dou, W. Li and J. Chen, *Sci. Adv.*, 2021, **7**, eabl3742.
- 33 Q. Xi, D. M. Zhou, Y. Y. Kan, J. Ge, Z. K. Wu, R. Q. Yu and J. H. Jiang, *Anal. Chem.*, 2014, **86**, 1361–1365.
- 34 X. Zuo, H. Zhang, Q. Zhu, W. Wang, J. Feng and X. Chen, *Biosens. Bioelectron.*, 2016, **85**, 464–470.
- 35 I. M. Khan, S. Niazi, Y. Yu, A. Mohsin, B. S. Mushtaq, M. W. Iqbal, A. Rehman, W. Akhtar and Z. Wang, *Anal. Chem.*, 2019, **91**, 14085–14092.
- 36 P. Wang, A. Wang, M. M. Hassan, Q. Ouyang, H. Li and Q. Chen, *Sens. Actuators, B*, 2020, **320**, 128434.
- 37 S. Eissa and M. Zourob, *Biosens. Bioelectron.*, 2017, **91**, 169–174.
- 38 M. Lettieri, O. Hosu, A. Adumitrachioaie, C. Cristea and G. Marrazza, *Electroanalysis*, 2020, **32**, 217–225.
- 39 Q. Qiu, X. Ni, T. Liu, Z. Li, X. An and X. Chen, *Analyst*, 2021, **146**, 6808–6814.